DALTON
FULL PAPER

On the inverse *trans* influence. Density functional studies of $[MOX_5]^{n-}$ (M = Pa, n = 2; M = U, n = 1; M = Np, n = 0; X = F, Cl or Br)

Emma O'Grady and Nikolas Kaltsoyannis

Department of Chemistry, University College London, 20 Gordon Street, London, UK WC1H 0AJ. E-mail: n.kaltsoyannis@ucl.ac.uk

Received 23rd October 2001, Accepted 28th November 2001
First published as an Advance Article on the web 7th February 2002

The geometric and electronic structures of $[MOX_5]^{n-}$ (M = Pa, n = 2; M = U, n = 1; M = Np, n = 0; X = F, Cl or Br) have been investigated using relativistic density functional theory. An inverse *trans* influence (*i.e.* in which the An–X_{cis} distances are longer than the An–X_{trans} bonds) is found in all cases, and there is good agreement with the experimental structure of $[UOCl_5]^-$. The O–An–X_{cis} angle is in all cases found to be very close to 90°, by contrast to analogous transition metal systems in which this angle is between 96° and 102°, and which display a regular *trans* influence. Molecular orbital arguments are presented to account for the difference in angle at the metal between the d- and f-block systems, and hence for the difference in their *trans* influence behaviour. Comparisons are drawn with previous explanations for the inverse *trans* influence in the title systems. Mayer bond orders are reported, and are used to understand further the metal–ligand interactions.

Introduction

The *trans* influence is a well established phenomenon in inorganic chemistry, to the point that it is standard material in most university level inorganic texts.[1,2] It is most commonly found in square planar and pseudo-octahedral transition metal complexes, in which tightly bound ligands selectively weaken (and lengthen) the bonds to ligands *trans* to their own position. It is the ground state analogue of the *trans* effect, a kinetic phenomenon in which ligands labilise ligands *trans* to themselves.

By contrast, certain pseudo-octahedral actinide complexes display the opposite trend in *cis* and *trans* bond lengths to that normally found in transition metal chemistry. In $[UOCl_5]^-$, for example, the bond between the uranium and the chlorine *trans* to the oxo group is 243.3 pm long, while the U–Cl_{cis} distance is 253.6 pm.[3] In 1992, Denning introduced the term *inverse trans influence* (ITI) to describe this phenomenon, and offered a 'naive, but pleasingly simple' explanation for its origins.[4]

In this contribution we report the results of relativistic density functional theory investigations of the geometric and electronic structures of $[MOX_5]^{n-}$ (M = Pa, n = 2; M = U, n = 1; M = Np, n = 0; X = F, Cl or Br), all of which are valence isoelectronic and which contain the metal in its group valency, *i.e.* the metal centres have the formal [Rn] configuration. We initially wished to see if our computational approach produced an ITI. As described below, we did indeed find this to be the case, and subsequently turned to an examination of the electronic structures of the title systems with a view to determining the origin of the ITI. Our findings are discussed with reference to the previous analysis offered by Denning.

The regular *trans* influence in pseudo-octahedral transition metal complexes has been studied theoretically for $[OsNCl_5]^{2-}$ by Lyne and Mingos,[5] and for *mer*-$[Ti(NR)Cl_2(NH_3)_3]$ (R = Bu^t, C_6H_5 and 4-$C_6H_4NO_2$) by Kaltsoyannis and Mountford.[6] The present studies of the ITI in the title systems are discussed with reference to these earlier investigations, and particular emphasis is placed on establishing the origin of the different *trans* influence behaviour of the d- and f-block complexes.

Computational details

All the calculations were performed on a Compaq XP1000 workstation using the Amsterdam Density Functional program suite.[7–11] An uncontracted double-zeta Slater-type orbital valence basis set was employed for the halogen atoms and oxygen, supplemented with a d polarisation function (ADF Type III). For the actinide atoms, ADF Type IV basis sets were used, which may be described as triple-zeta without polarisation functions (*i.e.* no g functions are included). Scalar relativistic corrections[12] were included *via* the ZORA method.[13,14] The frozen core approximation was employed, and relativistic frozen cores (calculated by the ADF auxiliary program 'Dirac') were used for oxygen (1s), fluorine (1s), chlorine (2p) and bromine (3d). This choice of frozen cores produces the same number of non-frozen valence atomic functions for all non-metallic elements (two s, two p, one d). For the actinide atoms, the size of the frozen core was varied as is discussed in the main text, but was most commonly up to and including the 5d orbitals, leaving four s, three p, three d and three f valence functions. The local density parameterisation of Vosko *et al.*[15] was employed. All of the geometry optimisations were conducted using C_{4v} symmetry constraints. Mulliken population analyses were performed.[16] Mayer bond orders were calculated from the ADF ascii output files using the MAYER program written by A. Bridgeman of the University of Hull.[17] Molecular orbital plots were generated using the MOLDEN program, written by G. Schaftenaar of the CAOS/CAMM Centre, Nijmegen, The Netherlands.[18] The same MOLDEN 'space' value (0.05) has been used for all plots. The ADF binary output files (TAPE21) were converted to MOLDEN format using the ADFrom99 program written by F. Mariotti of the University of Florence.[18]

Results and discussion

A Optimised geometries

The optimised geometries of all nine title systems are collected in Table 1. There are two calculated values for each bond

Table 1 Calculated (C_{4v} symmetry) and experimental geometries of $[MOX_5]^{n-}$ (M = Pa, n = 2; M = U, n = 1; M = Np, n = 0; X = F, Cl or Br). Data obtained with metal frozen cores excluding the 6p AOs are given in normal type, while those in which the metals' 6p AOs are included in the frozen core are in italics. Experimental data are given in brackets

	$[PaOF_5]^{2-}$	$[PaOCl_5]^{2-}$	$[PaOBr_5]^{2-}$	$[UOF_5]^{-}$	$[UOCl_5]^{-}$	$[UOBr_5]^{-}$	$[NpOF_5]$	$[NpOCl_5]$	$[NpOBr_5]$
r(An–O)/pm	189.7	183.3	182.4	183.0	179.9	179.4	175.8	175.6	175.8
	193.3	*186.2*	*185.1*	*185.0*	*181.0*	*180.5*	*181.3*	*178.9*	*179.0*
		(174(9))[a]			(176(1))[b]				
r(An–X_{trans})/pm	215.4	261.3	276.9	204.0	249.2	265.9	194.0	234.4	251.6
	220.2	*269.6*	*285.2*	*207.5*	*253.5*	*269.1*	*199.9*	*244.0*	*260.0*
		(242(3))[a]			(243.3(4))[b]				
r(An–X_{cis})/pm	219.9	264.9	280.2	208.7	253.2	269.4	200.5	241.1	257.9
	222.0	*270.5*	*285.8*	*210.5*	*255.9*	*271.0*	*203.3*	*246.9*	*262.1*
		(264 ± 0.05(5))[a]			(253.6(2))[b]				
Inverse *trans*	97.9	98.6	98.8	97.7	98.4	98.7	96.7	97.2	97.5
influence (%)	*99.2*	*99.7*	*99.8*	*98.6*	*99.1*	*99.3*	*98.3*	*98.8*	*99.2*
		(91.7)			(95.9)				
O–An–X_{cis}/°	93.0	90.7	90.4	91.7	90.3	89.9	89.4	88.5	88.4
		(91.6 av.)[a]			(89.7)[b]				

[a] Data from ref. 19. [b] Data from ref. 3.

length; those obtained with a metal frozen core excluding the 6p AOs (*i.e.* in which the metals' 5d AOs are the highest occupied core orbitals) are given in normal type, while those in which the metals' 6p AOs are included in the frozen core are in italics. Also given (in brackets) are the experimental data for $[PaOCl_5]^{2-}$ [19] and $[UOCl_5]^{-}$.[3]

The first point to note from Table 1 is that all of the calculations produce an ITI. We express this as a percentage, using the formula

$$\mathrm{ITI} = \frac{r(\mathrm{An}-\mathrm{X}_{trans})}{r(\mathrm{An}-\mathrm{X}_{cis})} \times 100\%$$

i.e. the smaller the percentage the larger the ITI. The calculated ITIs range from 96.7% for $[NpOF_5]$ (5d core) to 98.8% for $[PaOBr_5]^{2-}$. Comparison of the calculated with experimental data, however, shows that the calculated ITIs are smaller than those found experimentally, particularly for $[PaOCl_5]^{2-}$. Discrepancies between experimental solid state structures and calculated gas phase geometries are not uncommon, of course, but the differences between experiment and theory for $[PaOCl_5]^{2-}$ are such as to warrant further comment. We note that the crystal structure of $[NEt_4]_2[PaOCl_5]$ is not without its problems. There is a very large estimated standard deviation for the Pa–O distance (see Table 1); indeed, Brown and coworkers [19] noted the 'relatively small number of observed reflections' and the 'difficulty of accurately locating light atoms in structures containing actinide elements'. Furthermore, the Pa–Cl_{cis} distance of 264.9 pm is an average of values ranging from 259 pm to 272 pm, and the angular distortions around the Pa are also significant (the value of O–Pa–Cl_{cis} = 91.6° in Table 1 is an average of angles ranging from 83.4° to 98.8°). We therefore feel that $[UOCl_5]^{-}$ provides a more reliable comparison of experimental and theoretical structures. There is excellent agreement for the O–U–Cl_{cis} angle, and for the U–O and U–Cl_{cis} distances, although the calculation slightly overestimates (by *ca.* 6 pm) the U–Cl_{trans} bond length. It is this discrepancy which results in the calculated ITI being smaller than that found experimentally, but overall we feel that our computational approach does a very good job of reproducing the experimental data for $[UOCl_5]^{-}$.

All of the calculated geometries have been obtained using the local density approximation (LDA). A range of gradient corrections were tried, but resulted in longer An–O and An–X distances and smaller ITIs. It has been previously noted [20] that the LDA does a better job of reproducing the metal–ligand distances in classical Werner-type transition metal complexes (*i.e.* ones featuring anionic ligands with metals in high oxidation states) than does the generalised gradient approximation, and the same appears true for the title systems. We have therefore decided to analyse the electronic structures at the LDA geometries, on the grounds that these values are closer to the (admittedly limited) experimental values.

Table 2 Symmetries of the valence pσ and pπ oxygen and halogen AO combinations in pseudo-octahedral $[MOX_5]^{n-}$ (C_{4v} symmetry)

	Oxygen	*cis* Halogen	*trans* Halogen
Valence pσ	a_1	$a_1 + b_1 + e$	a_1
Valence pπ	e	$a_1 + a_2 + b_1 + b_2 + 2e$	e

There are a number of trends in the calculated ITIs. For a given metal, the ITI decreases in the order F > Cl > Br. Keeping the halogen fixed but changing the metal produces an ITI which increases in the order Pa < U < Np. It is also noticeable that the ITIs for the chloride and bromide of a given metal are quite similar, with that of the fluoride being larger. We return to these trends below.

B Valence molecular orbital structure

The occupied valence MOs of $[MOX_5]^{n-}$ (M = Pa, n = 2; M = U, n = 1; M = Np, n = 0; X = F, Cl or Br) are made up predominantly from the oxygen 2p and halogen valence p AOs. These AOs fall into two types; those of σ symmetry with respect to the metal–ligand axes and those of π symmetry along these vectors. Group theoretical analysis reveals that these AOs transform in C_{4v} as indicated in Table 2. These irreducible representations (irreps) are the symmetries of the AO basis combinations and hence of the expected valence MOs, and examination of the electronic structures of all nine title systems reveals that the valence region does indeed consist solely of MOs with the symmetries indicated in Table 2.

We now examine the valence MO structure of one of the title systems—$[UOBr_5]^{-}$ (U 5d core)—in more detail. We have chosen this system because the bonding character of the a_1 and e symmetry MOs is easiest to see; in some of the other molecules there is greater mixing of orbitals within a given symmetry type, although the principal bonding character is rarely obscured. Fig. 1 presents a valence MO energy level and composition diagram for $[UOBr_5]^{-}$. The bonding character of each MO is also given. There are several points to note from this figure. First, many of the MOs have a significant uranium content (as high as 32% in the $8a_1$ level). This uranium character derives from f, d and p AOs, and indicates appreciable covalency. Second, the primary U–O bonding MOs (3e and $6a_1$) are separated from the other levels by nearly 1 eV, reflecting the relative electronegativities of oxygen and bromine. Third, the

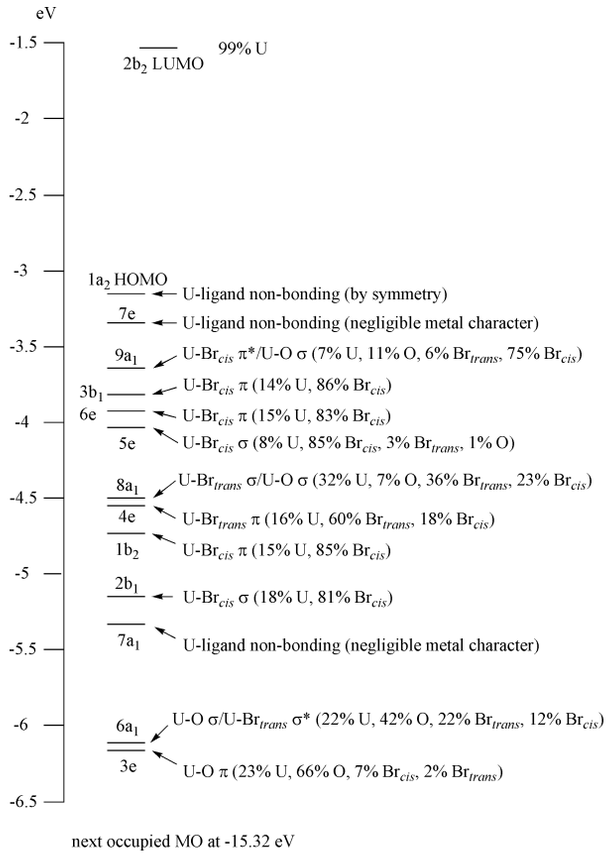

Fig. 1 Valence molecular orbital and composition diagram for $[UOBr_5]^-$.

U–Br MOs are primarily the $2b_1$–$9a_1$ levels, and are mainly metal–halogen bonding.

The calculated ITI in $[UOBr_5]^-$ is 98.7%, with the U–Br_{cis} bonds being 3.5 pm longer than the U–Br_{trans}. This ITI may in principle be caused by many factors, *e.g.* slightly weaker π bonding between the metal and *cis* halogens or stronger σ bonding to the *trans* ligands. It is, therefore, perhaps optimistic to expect that examination of the valence electronic structure of $[UOBr_5]^-$ on an orbital by orbital basis will produce a definitive explanation for the ITI, as there might in principle be contributions to it from the electrons in many MOs. Having said that, there are two MOs which differ in character from all the rest, and which may well provide an explanation for the ITI trends noted in the previous section. All of the MOs $2b_1$–$3b_1$ are U–Br bonding. However, the $6a_1$ level is antibonding between uranium and the *trans* bromines while the $9a_1$ orbital is antibonding between the metal and the *cis* halogens. Three dimensional representations of these two MOs are shown in Fig. 2. It is reasonable to suggest that the extent of the metal–halogen antibonding in these MOs will affect the magnitude of the ITI.

In section A, we noted that the fluoride of a given metal has a greater ITI than either the chloride or bromide. An explanation for this presents itself from analysis of the compositions of the $6a_1$ and $9a_1$ orbitals of all nine title species, given in Table 3. Recalling that the $6a_1$ of $[UOBr_5]^-$ is antibonding between the metal and the *trans* bromines, it is noticeable that the metal involvement in this orbital decreases in the order Br > Cl > F for a given metal, *i.e.* the M–X_{trans} antibonding due to the electrons in the $6a_1$ MO is greatest for X = Br and least for X = F. This may be illustrated by comparison of Fig. 2(a) with Fig. 3, which shows the $6a_1$ level of $[UOF_5]^-$. This latter MO is different in character from the $6a_1$ level of $[UOBr_5]^-$ in that it (a) has a much greater contribution from the *cis* fluorines (see Table 3 also), (b) is An–O antibonding and (c) has essentially no U–F_{trans} interactions, *i.e.* it is much less An–X_{trans} antibonding than the analogous MO of the bromine system.

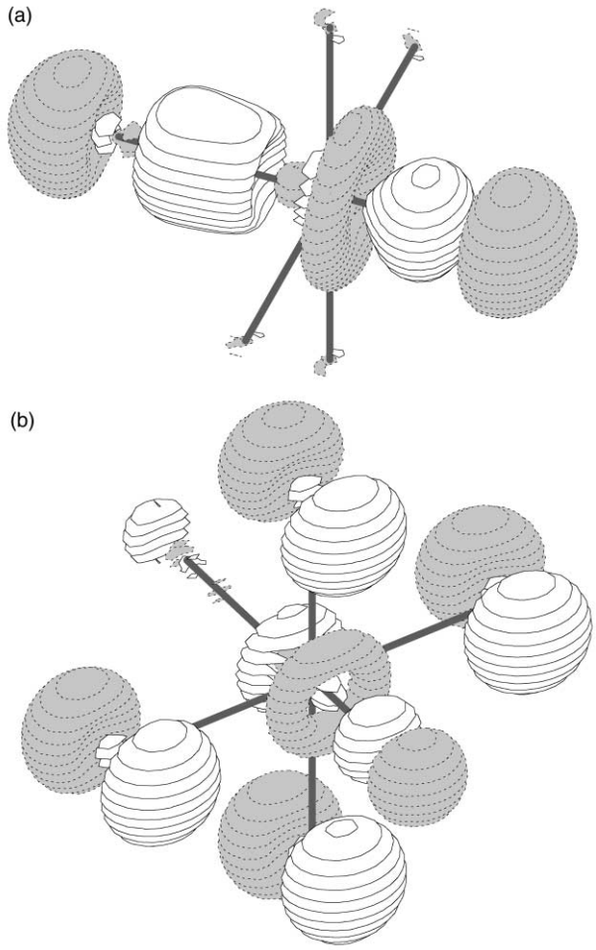

Fig. 2 Three-dimensional representations of the (a) $6a_1$ and (b) $9a_1$ molecular orbitals of $[UOBr_5]^-$. In both plots the molecule is oriented with the oxygen atom to the right and front.

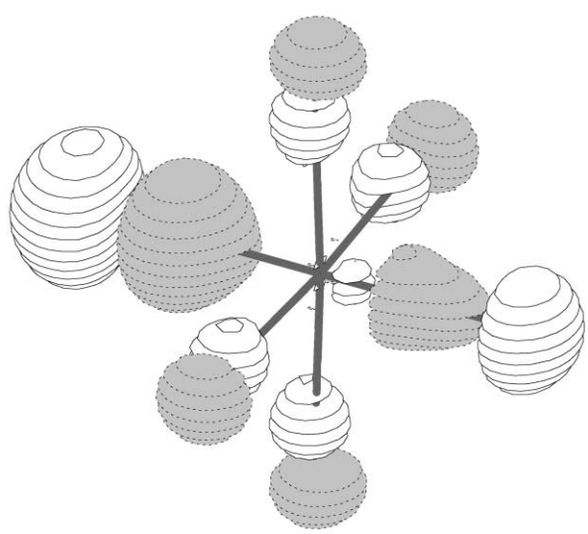

Fig. 3 Three-dimensional representation of the $6a_1$ molecular orbital of $[UOF_5]^-$. The molecule is oriented with the oxygen atom to the right.

By contrast to the $6a_1$ level, moving from X = Br to X = F produces a significant increase in the metal content of the $9a_1$ MO. This orbital is antibonding between the metal and the *cis* halogens, and thus replacement of Br by F leads to increased An–X_{cis} antibonding in this orbital. This is illustrated by the $9a_1$ level of $[NpOF_5]$ in Fig. 4 (compare with the $9a_1$ MO of $[UOBr_5]^-$ in Fig. 2(b)).

In summary, replacement of Br by F for any given metal leads to a reduction in the An–X_{trans} antibonding character of

Table 3 Composition (%, Mulliken analysis) of the $6a_1$ and $9a_1$ MOs of $[MOX_5]^{n-}$ (M = Pa, $n = 2$; M = U, $n = 1$; M = Np, $n = 0$; X = F, Cl or Br)

	Orbital	Metal	Oxygen	*trans* Halogen	*cis* Halogen
$[PaOF_5]^{2-}$	$6a_1$	1 f_{z^3}, 8 d_{z^2}	9	49	29
	$9a_1$	18 f_{z^3}, 3 d_{z^2}, 8 p_z	49	6	13
$[PaOCl_5]^{2-}$	$6a_1$	13 d_{z^2}, 1 p_z	25	38	20
	$9a_1$	15 f_{z^3}, 1 d_{z^2}, 6 p_z	31	12	33
$[PaOBr_5]^{2-}$	$6a_1$	2 f_{z^3}, 14 d_{z^2}, 2 p_z	35	31	14
	$9a_1$	9 f_{z^3}, 4 p_z	22	12	51
$[UOF_5]^{-}$	$6a_1$	2 f_{z^3}, 10 d_{z^2}	11	51	24
	$9a_1$	22 f_{z^3}, 1 d_{z^2}, 11 p_z	40	4	24
$[UOCl_5]^{-}$	$6a_1$	2 f_{z^3}, 14 d_{z^2}	33	30	17
	$9a_1$	9 f_{z^3}, 4 p_z	18	8	60
$[UOBr_5]^{-}$	$6a_1$	5 f_{z^3}, 14 d_{z^2}, 3 p_z	42	22	12
	$9a_1$	5 f_{z^3}, 2 p_z	11	6	75
$[NpOF_5]$	$6a_1$	2 f_{z^3}, 10 d_{z^2}	16	50	20
	$9a_1$	23 f_{z^3}, 7 p_z	18	3	46
$[NpOCl_5]$	$6a_1$	5 f_{z^3}, 13 d_{z^2}	39	24	15
	$9a_1$	10 f_{z^3}, 5 p_z	10	6	67
$[NpOBr_5]$	$6a_1$	9 f_{z^3}, 12 d_{z^2}, 1 p_z	44	20	11
	$9a_1$	6 f_{z^3}, 4 p_z	8	5	76

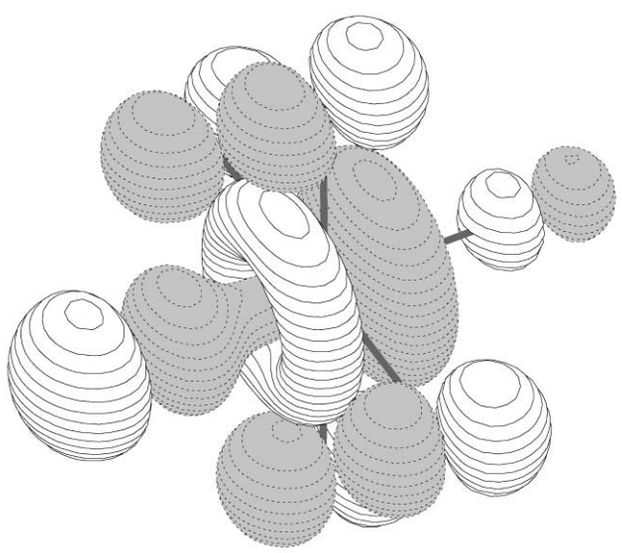

Fig. 4 Three-dimensional representation of the $9a_1$ molecular orbital of $[NpOF_5]$. The molecule is oriented with the oxygen atom to the left.

the $6a_1$ MO and an increase in the An–X_{cis} antibonding character of the $9a_1$ level. This should therefore lead to a shortening of the An–X_{trans} bonds and an increase in the An–X_{cis} distances, *i.e.* to an increase in ITI.

The data in Table 3 also provide an explanation for the increase in ITI from Pa to U and Np. Focusing on the fluorides, it is noticeable that the metal and *trans* fluorine contributions to the $6a_1$ MO are largely unaltered on moving from $[PaOF_5]^{2-}$ to $[NpOF_5]$. The same is true of the metal contribution to the $9a_1$ level. However, the *cis* fluorine content of this orbital increases very significantly, *i.e.* the An–F_{cis} antibonding character of the $9a_1$ MO is substantially larger for $[NpOF_5]$ than $[PaOF_5]^{2-}$, leading to a larger ITI in the former. Similar trends can be identified in the compositions of the $6a_1$ and $9a_1$ MOs of the chlorides and bromides, although they are perhaps less clear cut than is the case for the fluorides.

C The relationship of the present analysis to the previous explanation of Denning

As indicated in the Introduction, we are not the first to attempt an explanation of the ITI. Denning put forward a 'naive, but pleasingly simple' explanation,[4] and we were keen to see how our results related to this. We now summarise Denning's argument:

Consider the tightly bound ligand (in the case of the title molecules the oxo group) to be an anion. There is an electrostatic interaction between the anion and the core electrons of the metal atom, inducing a polarisation of the latter. The nature of this core polarisation is critically dependent upon the relative parity of the highest occupied core orbitals and the lowest unoccupied metal valence AOs. If these sets of AOs have opposite parity, as for early transition metals where the core AOs are p and the valence d, the polarisation is predominantly dipolar, leading to a build up of negative charge in the position *trans* to the tightly bound ligand. This results in greater repulsion between the metal and the ligand in the *trans* position than between the metal and the *cis* ligand, resulting in a regular *trans* influence. By contrast, if the core AOs are p and the valence f (as in the title systems) the polarisation is predominantly quadrupolar, with a build up of negative charge in the *cis* position and hence an ITI.

In another publication[21] Denning and co-workers wrote: 'In alternative terminology, the involvement of the 6p pseudo-core orbitals in the σ bond to the strongly bound ligand leads to hybridisation with, and a transfer of charge to, the f orbitals, leaving a partial core hole in the 6p orbital directed toward the *trans* position. This core hole removes charge from the antibonding 6p shell, and can therefore selectively enhance 5f overlap in the *trans* position.'

As indicated above, we wanted to see how our results relate to these previous explanations; indeed, Denning's explanations were the initial motivation behind the present study. As we now discuss, however, it is not always clear how our data relate to Denning's arguments.

Denning's explanations centre around the actinide 6p semi-core AOs. One might therefore imagine that placement of the actinide 6p AOs into the frozen core should cause the disappearance of the ITI, as frozen orbitals cannot mix or change their energy during the SCF and geometry cycles. The data in Table 1 suggest that there is indeed a reduction in the ITIs in all cases on freezing the 6p AOs, but that small ITIs remain. This suggests that the metals' 6p AOs play a role in determining the magnitude of the calculated ITIs, but also that there must be at least one other factor involved.

In section B we suggested that the extent of An–X_{cis} antibonding in the $9a_1$ MO is important in determining the magnitude of the ITI. This orbital may also help to evaluate Denning's 'alternative terminology' explanation. † Focusing on the fluoride systems, the $9a_1$ level is strongly An–O σ bonding (see Table 3 and Fig. 4). The data in Table 3 reveal that there is a metal p_z contribution to this MO, with $[PaOF_5]^{2-}$ and $[NpOF_5]$ having similar contributions and that in $[UOF_5]^{-}$ being slightly

† We focus on this form of Denning's explanation because (a) it is easier to relate to our orbital approach and (b) we have no method of evaluating directly the polarisation of the actinide cores.

larger (the 11% p_z contribution to the $9a_1$ MO of $[UOF_5]^-$ is the largest in any valence MO of the title systems). It might be expected, therefore, that if Denning's explanation is complete, the ITI would be greatest for $[UOF_5]^-$ because the An–O σ level has the most actinide 6p character. The ITI in the fluoride systems, however, is largest for $[NpOF_5]$, which has the smallest p_z contribution to the $9a_1$ level. We have argued that it is the larger $An–X_{cis}$ antibonding character of the $9a_1$ MO of $[NpOF_5]$ in comparison with the equivalent protactinium and uranium orbitals which produces the larger ITI in the neptunium system, and it would appear that this effect is more significant than the involvement of the 6p AOs in the An–O σ level.

The involvement of the 6p AOs in the valence electronic structure of $[UO_2]^{2+}$ is the reason why the valence σ_u MO of this system is significantly less stable than the other valence levels.[22] A concomitant effect is the generation of a hole in the 6p shell, *i.e.* there are no longer exactly six 6p electrons associated with the metal centre. Given that there is an admixture of $6p_z$ into some of the valence MOs of a_1 symmetry in the title systems, it would be expected that 6p core holes would result. This is indeed the case, the metal p AO populations being 5.73, 5.86 and 5.23 respectively for $[PaOF_5]^{2-}$, $[UOF_5]^-$ and $[NpOF_5]$. Unfortunately the trend in these populations does not fit with the trend in ITIs, and a similar lack of correlation is found in the chlorides and bromides (*e.g.* the metal p population in $[PaOBr_5]^{2-}$ is less than in $[PaOCl_5]^{2-}$, while for $[UOCl_5]^-$ and $[UOBr_5]^-$ the p populations are slightly larger than 6 (presumably reflecting the very small 7p contribution to some of the valence AOs)).

We therefore conclude that the existence and magnitude of the ITI in $[MOX_5]^{n-}$ (M = Pa, $n = 2$; M = U, $n = 1$; M = Np, $n = 0$; X = F, Cl or Br) are not fully explained by analysis of factors associated with the metals' 6p AOs. It is clear that these AOs play a role in the ITI, but that they do not provide a complete explanation.

D Comparison with the regular *trans* influence in pseudo-octahedral $[OsNCl_5]^{2-}$

As noted in the Introduction, the regular *trans* influence is common in d-block chemistry. $[OsNCl_5]^{2-}$, which is clearly closely related to the title systems, is a good example of a transition metal complex in which there is a pronounced *trans* influence, and has been studied theoretically within the last few years.[5,6] Lyne and Mingos found that the second HOMO (the 4e MO in reference 5) is π bonding between the metal and the nitrido group but π antibonding between the metal and the *cis* chlorines. Increasing the $N–Os–Cl_{cis}$ angle above 90° causes this orbital to become more bonding between the metal and nitrogen, while reducing the $Os–Cl_{cis}$ antibonding character. There is therefore an orbital driving force toward increase of the $N–Os–Cl_{cis}$ angle. Tempering this drive to bending are two further MOs ($2a_1$ and 3e in reference 5). The $2a_1$ MO has contributions from p_π on the *cis* chlorines and p_σ from the *trans* chlorine. These are out of phase with one another and hence increasing the $N–Os–Cl_{cis}$ angle destabilises the $2a_1$ MO as the *cis*/*trans* antibonding overlap increases. The 3e MO is primarily Cl_{cis} and Cl_{trans} p_π in character, and is also destabilised as the $N–Os–Cl_{cis}$ angle increases. The final $N–Os–Cl_{cis}$ angle is a competition between the $2a_1$, 3e and 4e electrons, and was found to be 96° by Lyne and Mingos.

This orbital analysis also led Lyne and Mingos to an explanation for the regular *trans* influence in $[OsNCl_5]^{2-}$; as the $N–Os–Cl_{cis}$ angle increases above 90°, non-bonded repulsions between the *cis* and *trans* chlorine atoms result in a lengthening of the $Os–Cl_{trans}$ distance.

Why, then, does $[OsNCl_5]^{2-}$ exhibit a regular *trans* influence while the title complexes have an ITI? The $N/O–M–X_{cis}$ angle is clearly of central importance, in that the larger it is the larger the repulsions between the *cis* and *trans* halogens and hence the more the system should exhibit a regular *trans* influence. The $O–An–X_{cis}$ angles of the title complexes are all very close to 90° (Table 1) suggesting that, if there is an orbital driving force toward increasing this angle similar to that in the 4e MO of $[OsNCl_5]^{2-}$, it is outweighed by other interactions which favour 90°.

Table 4 Optimised $U–Br_{cis}$ and $U–Br_{trans}$ distances in constrained geometry optimisations of $[UOBr_5]^-$

	$O–U–Br_{cis}$ angle = 90°	$O–U–Br_{cis}$ angle = 102°
$U–Br_{cis}$/pm	269.4	270.5
$U–Br_{trans}$/pm	265.9	272.7
ITI (%)	98.7	100.8

In order to probe this more fully, we have conducted a series of constrained geometry optimisations of $[UOBr_5]^-$ in which the $O–U–Br_{cis}$ angle is increased in 1° steps from 90° to 102°, all the bond lengths being allowed to optimise at each angle. The $U–Br_{cis}$ and $U–Br_{trans}$ distances at $O–U–Br_{cis}$ = 90° and 102° are given in Table 4, from which it is clear that increasing the $O–U–Br_{cis}$ angle not only reduces the ITI but, by 102°, produces a regular *trans* influence.

Examination of the changes in the energies of the valence MOs reveals that there are three which experience energy changes of $> \pm 0.07$ eV as the $O–U–Br_{cis}$ angle changes from 90° to 102°. These are as follows: 4e, −0.14 eV; $8a_1$, +0.23 eV; 7e, +0.57 eV. The destabilisation of the $8a_1$ and 7e MOs is clearly quite substantial. These two orbitals are similar to the $2a_1$ and 3e levels of $[OsNCl_5]^{2-}$, and are illustrated in Fig. 5 for the complex with $O–U–Br_{cis}$ = 90° (note that this geometry with this constraint is practically identical to the fully optimised geometries given in Table 1). Fig. 5 reveals why they are destabilised on increasing the $O–U–Br_{cis}$ angle; both are clearly antibonding between the *cis* and *trans* bromines. The energetic cost to these MOs of increasing the $O–U–Br_{cis}$ angle is much more than is gained through the stabilisation of the 4e‡ MO, and hence the $O–U–Br_{cis}$ angle in the fully optimised geometry of $[UOBr_5]^-$ is very close to 90°.

In $[OsNCl_5]^{2-}$, the orbital driving force toward bending is provided by the 4e MO which, as described above, is Os–N π bonding and $Os–Cl_{cis}$ π antibonding. Increasing the $N–Os–Cl_{cis}$ angle strengthens the Os–N bonding and alleviates the $Os–Cl_{cis}$ antibonding. What, if any, is the equivalent MO in $[MOX_5]^{n-}$ (M = Pa, $n = 2$; M = U, $n = 1$; M = Np, $n = 0$; X = F, Cl or Br) and what is the dependence of its energy upon the $O–An–X_{cis}$ angle? As discussed in sections B and C, we attribute the ITIs in the fully optimised structures of the title systems partly to $An–X_{cis}$ π antibonding in the $9a_1$ MOs, shown for $[UOBr_5]^-$ and $[NpOF_5]$ in Figs. 2(b) and 4 respectively. It would be expected that increasing the $O–An–X_{cis}$ angle would alleviate the $An–X_{cis}$ π antibonding and stabilise the orbital. This is indeed found to be the case, but for $[UOBr_5]^-$ the $9a_1$ level is stabilised by only 0.05 eV between 90° and 102°, *i.e.* the stabilisation of this MO is nothing like big enough to overcome the resistance to bending in the $8a_1$ and 7e MOs.§ Lyne and Mingos do not report the extent to which the 4e level of $[OsNCl_5]^{2-}$ is stabilised, but the analogous orbital of $[Ti(NBu^t)Cl_2(NH_3)_3]$

‡ Note that the 4e MO of $[UOBr_5]^-$ is not the same as the 4e level of $[OsNCl_5]^{2-}$!

§ We noted earlier that the $9a_1$ MO of $[UOBr_5]^-$ is not strongly $U–Br_{cis}$ antibonding, and that replacing the Br with lighter halides leads to an increase in the antibonding character of this orbital. We have performed constrained geometry optimisations on $[NpOCl_5]$ for $O–Np–Cl_{cis}$ = 90° and 102° and found that the $9a_1$ MO in this system is stabilised by 0.19 eV, significantly more than in $[UOBr_5]^-$. However, in $[NpOCl_5]$ the 7e level is destabilised by 0.45 eV, and hence even with greater $An–X_{cis}$ π antibonding the orbital driving force toward bending in $[NpOCl_5]$ is insufficient to overcome the overall orbital preference for the $O–Np–Cl_{cis}$ angle to be 90°.

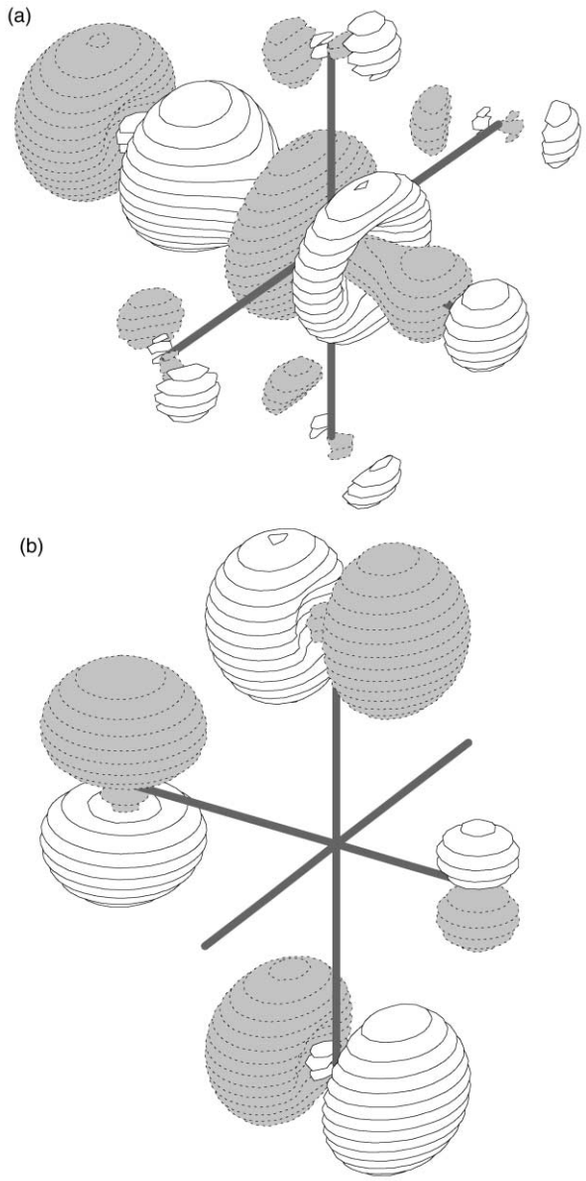

Fig. 5 Three-dimensional representations of the (a) $8a_1$ and (b) 7e (one component only) molecular orbitals of $[UOBr_5]^-$. The geometry has been constrained to have a O–U–Br_{cis} angle of 90°. In both plots the molecule is oriented with the oxygen atom to the right.

(another pseudo-octahedral transition metal system displaying a regular *trans* influence) is stabilised by more than 0.4 eV between N–Ti–Cl_{cis} = 90° and 102°.[6]

Why, then, does the $9a_1$ of $[MOX_5]^{n-}$ (M = Pa, n = 2; M = U, n = 1; M = Np, n = 0; X = F, Cl or Br) not provide the same orbital driving force toward bending as found in other transition metal complexes? The answer may well lie in the fact that the $9a_1$ MO of the title systems, by virtue of its An f_{z^3} character, is σ bonding between the metal and the tightly bound oxo ligand, not π bonding as is the case for the analogous MOs of other transition metal systems. Hence a reduction in An–X_{cis} π antibonding on increasing the O–An–X_{cis} angle cannot be accompanied by a strengthening of the An–O π bond in this MO. We suggest that this is the reason for the reduced stabilisation of the An–X_{cis} π antibonding MO in the title systems, and hence ultimately for the O–An–X_{cis} angle to be very close to 90°.

The 4e MO of $[UOBr_5]^-$ is stabilised the most on bending, by 0.14 eV as noted above. Lyne and Mingos make no mention of an analogous orbital in $[OsNCl_5]^{2-}$. This level is predominantly An–X_{trans} π bonding in the title systems, although there is some An–X_{cis} bonding character as well. As the O–An–X_{cis} angle increases, the 4e level stabilises on account of a direct bonding interaction between the *cis* and *trans* halogens. This stabilisation, however, is clearly insufficient to overcome the destabilisation of the $8a_1$ and 7e orbitals.

E Mayer bond orders

In this section we change focus slightly and turn our attention to another approach which we have used to gain insight into the ITIs and the electronic structures of the title systems in general. Mayer Bond Orders (MBOs)[23,24] seek to quantify the interaction between two atoms in a molecule in chemically familiar ways, in terms of, for example, single and multiple, σ and π bonding. They have a potential advantage over the individual MO approach used above in that they contain all of the contributions to a bond between two atoms, *i.e.* they take account of all bonding and antibonding interactions in a single number. MBOs have been applied to a variety of inorganic systems by Bridgeman and co-workers.[25]

The calculated MBOs of $[MOX_5]^{n-}$ (M = Pa, n = 2; M = U, n = 1; M = Np, n = 0; X = F, Cl or Br) are given in Table 5. The total bond orders between bonded atoms are given, and are broken down into contributions from the symmetry subspecies of C_{4v} (there are no metal AOs which transform as a_2 in C_{4v}, and thus no a_2 bond order). There are several points to note from these data:

1. In all cases bar $[UOF_5]^-$ and $[NpOF_5]$, the An–X_{cis} bond orders are less than the An–X_{trans}. It is well established that there is generally good correlation between MBO and bond length,[25] and hence these data reflect the ITI of the title systems. Bridgeman and co-workers noted that the calculation of MBOs for element–fluorine bonds can be troublesome, probably because of the high ionicity of the bonding. It is noticeable that by far the largest metal–halogen charge differences (Mulliken analysis) in our systems are found in $[UOF_5]^-$ and especially $[NpOF_5]$, *i.e.* those species for which the MBO does not reflect the ITI.

2. The An–O bond order is remarkably constant across the nine systems, at around 1.9 in all cases. This is interesting because although the formal An–O bond order in actinyl ions and actinyl ion complexes is 3, the An–O bond is almost always written as a double bond.[22,26] At first glance our data appear to support this latter description of the An–O bond. However, Bridgeman and co-workers noted that MBOs are often underestimated in multiply bonded systems calculated with ADF frozen core basis sets[25] (by as much as 0.5 in comparison with similar quality all-electron Gaussian Type Orbital bases) and we suggest that this is also happening in the present study, *i.e.* that the 'true' An–O bond orders are significantly greater than 2.

3. Keeping the metal fixed and altering the halogen from fluorine to bromine produces in all cases an increase in the An–X MBOs. This is unsurprising given the electronegativity decrease down Group 17, and reflects greater metal–ligand covalency with increasing halogen atomic number. Interestingly, the breakdown of the total bond order by irreps suggests that this increased covalency is primarily localised in the σ framework. Thus, for An–X_{trans} the bond orders in the e irrep (π with respect to the An–X_{trans} bond) increase much less than those in the a_1 irrep as the halogen becomes heavier. The situation is more complicated for An–X_{cis} as the a_1, b_1 and e irreps contain contributions from both σ and π interactions. The bond orders in all of these irreps increase as the halogen becomes heavier. However, the bond orders of the b_2 irrep (solely An–X_{cis} π in character) remain essentially constant, suggesting that the An–X_{cis} MBO increase is also due to greater σ covalency.

4. For a given halogen, altering the metal from protactinium to neptunium produces an increase in MBO. This is presumably a reflection of the shorter metal–halogen bond lengths for the heavier actinides (the metals' atomic and ionic radii decrease

Table 5 Mayer bond orders in $[MOX_5]^{n-}$ (M = Pa, $n = 2$; M = U, $n = 1$; M = Np, $n = 0$; X = F, Cl or Br)

	$[PaOF_5]^{2-}$			$[PaOCl_5]^{2-}$			$[PaOBr_5]^{2-}$		
	Pa–O	Pa–F_{cis}	Pa–F_{trans}	Pa–O	Pa–Cl_{cis}	Pa–Cl_{trans}	Pa–O	Pa–Br_{cis}	Pa–Br_{trans}
a_1	0.67	0.10	0.34	0.64	0.14	0.58	0.62	0.15	0.65
b_1	0.0	0.16	0.0	0.0	0.23	0.0	0.0	0.25	0.0
b_2	0.0	0.11	0.0	0.0	0.11	0.0	0.0	0.11	0.0
e	1.18	0.37	0.44	1.30	0.45	0.44	1.31	0.48	0.44
Total	1.85	0.74	0.78	1.94	0.93	1.02	1.93	0.99	1.09
	$[UOF_5]^{-}$			$[UOCl_5]^{-}$			$[UOBr_5]^{-}$		
	U–O	U–F_{cis}	U–F_{trans}	U–O	U–Cl_{cis}	U–Cl_{trans}	U–O	U–Br_{cis}	U–Br_{trans}
a_1	0.66	0.08	0.32	0.61	0.15	0.59	0.60	0.17	0.66
b_1	0.0	0.19	0.0	0.0	0.28	0.0	0.0	0.30	0.0
b_2	0.0	0.11	0.0	0.0	0.12	0.0	0.0	0.12	0.0
e	1.24	0.41	0.46	1.32	0.58	0.60	1.30	0.61	0.60
Total	1.88	0.79	0.78	1.93	1.13	1.19	1.90	1.20	1.26
	$[NpOF_5]$			$[NpOCl_5]$			$[NpOBr_5]$		
	Np–O	Np–F_{cis}	Np–F_{trans}	Np–O	Np–Cl_{cis}	Np–Cl_{trans}	Np–O	Np–Br_{cis}	Np–Br_{trans}
a_1	0.61	0.05	0.37	0.61	0.13	0.80	0.59	0.16	0.90
b_1	0.0	0.23	0.0	0.0	0.35	0.0	0.0	0.37	0.0
b_2	0.0	0.10	0.0	0.0	0.13	0.0	0.0	0.13	0.0
e	1.30	0.55	0.50	1.32	0.83	0.70	1.32	0.89	0.72
Total	1.91	0.93	0.87	1.93	1.44	1.50	1.91	1.55	1.62

quite significantly in the order Pa > U > Np[27]). For An–X_{trans} the increase in bond order is in both the a_1 and e irreps, while for An–X_{cis} it is mainly in the b_1 and e symmetry subspecies. Given that all of these irreps span both σ and π, it is not possible to characterise the MBO increases as being due either to mainly increased σ bonding or to predominantly increased π bonding.

Summary and conclusions

In this contribution we have used relativistic DFT to show that the gas phase structures of $[MOX_5]^{n-}$ (M = Pa, $n = 2$; M = U, $n = 1$; M = Np, $n = 0$; X = F, Cl or Br) display an ITI. Agreement with solid state experimental geometries is excellent for $[UOCl_5]^-$ but less good for $[PaOCl_5]^{2-}$, although this latter discrepancy may well be due to experimental difficulties rather than computational inaccuracies. We have used arguments based on valence MO structure to explain why the O–An–X_{cis} angles are very close to 90° in all cases. Specifically, we find that the alleviation of An–X_{cis} π antibonding on increasing the O–An–X_{cis} angle is insufficient to overcome the concomitant destabilisation of the X_{cis}/X_{trans} antibonding MOs. By contrast, in analogous transition metal complexes, M–X_{cis} π antibonding alleviation is accompanied by increased π bonding between the metal and the tightly bound atom, and this dual effect more than compensates for the increased X_{cis}/X_{trans} antibonding on increasing the angle at the metal. The increase in the *cis* angle at the metal in the transition metal systems leads to a regular *trans* influence through *cis*/*trans* halogen repulsion, an effect which is minimised in the title systems because the *cis* angle is *ca*. 90°.

We have also developed MO arguments based primarily upon the relative extent of metal–halogen antibonding in the $6a_1$ and $9a_1$ levels to explain why there is an ITI at the fully optimised geometries of the title systems, and to account for the variations in ITI as both actinide and halogen are varied. Comparison of our ITI explanations with previous ones offered by Denning is not entirely satisfactory, in that although we conclude that, as suggested by Denning, the actinide 6p semi-core orbitals play a role in the ITI, we find that they are not the sole determining factor.

Acknowledgements

We are grateful to University College London for a Teaching Assistantship to E. O'G. and to Professor Bob Denning for helpful comments.

References

1 N. N. Greenwood and A. Earnshaw, *Chemistry of the Elements*, Pergamon Press, Oxford, 2nd edn., 1997.
2 C. E. Housecroft and A. G. Sharpe, *Inorganic Chemistry*, Prentice Hall, Harlow, 2001.
3 J. F. de Wet and J. G. H. du Preez, *J. Chem. Soc., Dalton Trans.*, 1978, 592.
4 R. G. Denning, *Struct. Bonding (Berlin)*, 1992, **79**, 215.
5 P. D. Lyne and D. M. P. Mingos, *J. Chem. Soc., Dalton Trans.*, 1995, 1635.
6 N. Kaltsoyannis and P. Mountford, *J. Chem. Soc., Dalton Trans.*, 1999, 781.
7 ADF2000, Department of Theoretical Chemistry, Vrije Universiteit, Amsterdam, 2000.
8 E. J. Baerends, D. E. Ellis and P. Ros, *Chem. Phys.*, 1973, **2**, 41.
9 L. Versluis and T. Ziegler, *J. Chem. Phys.*, 1988, **88**, 322.
10 G. te Velde and E. J. Baerends, *J. Comput. Phys.*, 1992, **99**, 84.
11 C. Fonseca Guerra, J. G. Snijders, G. te Velde and E. J. Baerends, *Theor. Chem. Acc.*, 1998, **99**, 391.
12 N. Kaltsoyannis, *J. Chem. Soc., Dalton Trans.*, 1997, 1.
13 E. van Lenthe, R. van Leeuwen, E. J. Baerends and J. G. Snijders, *Int. J. Quantum Chem.*, 1996, **57**, 281.
14 E. van Lenthe, J. G. Snijders and E. J. Baerends, *J. Chem. Phys.*, 1996, **105**, 6505.
15 S. H. Vosko, L. Wilk and M. Nusair, *Can. J. Phys.*, 1980, **58**, 1200.
16 R. S. Mulliken, *J. Chem. Phys.*, 1955, **23**, 1833; R. S. Mulliken, *J. Chem. Phys.*, 1955, **23**, 1841; R. S. Mulliken, *J. Chem. Phys.*, 1955, **23**, 2328; R. S. Mulliken, *J. Chem. Phys.*, 1955, **23**, 2343.
17 A. J. Bridgeman, MAYER, University of Hull, 2001.
18 For details of both MOLDEN and ADFrom99, the reader is directed to http://www.caos.kun.nl/~schaft/molden/molden.html.
19 D. Brown, C. T. Reynolds and P. T. Moseley, *J. Chem. Soc., Dalton Trans.*, 1972, 857.
20 M. R. Bray, R. J. Deeth, V. J. Paget and P. D. Sheen, *Int. J. Quantum Chem.*, 1997, **61**, 85.
21 J. M. Bartleet, R. G. Denning and I. D. Morrison, *Mol. Phys.*, 1992, **75**, 601.
22 N. Kaltsoyannis, *Inorg. Chem.*, 2000, **39**, 6009.
23 I. Mayer, *Chem. Phys. Lett.*, 1983, **97**, 270.
24 I. Mayer, *Int. J. Quantum Chem.*, 1984, **26**, 151.
25 A. J. Bridgeman, G. Cavigliasso, L. R. Ireland and J. Rothery, *J. Chem. Soc., Dalton Trans.*, 2001, 2095.
26 N. Kaltsoyannis and P. Scott, *The f elements*, Oxford University Press, Oxford, 1999.
27 J. Emsley, *The Elements*, Oxford Univeristy Press, Oxford, 2nd edn., 1991.